Mössbauer Studies of Fe^{2+} in Iron Langbeinites and other Crystals with Langbeinite Structure

M. Windhaus, B. D. Mosel, and W. Müller-Warmuth

Institut für Physikalische Chemie der Westfälischen Wilhelms-Universität, Schlossplatz 4/7, D-48149 Münster

Z. Naturforsch. **53a,** 27–37 (1998); received January 21, 1998

^{57}Fe Mössbauer spectra have been measured at various temperatures between 4.2 K and 300 K for iron langbeinites $A_2Fe_2(SO_4)_3$ with A = K, NH_4, Rb, Tl and magnesium, manganese and cadmium langbeinites doped with Fe^{2+}. The spectra revealed several contributions whose isomer shifts and quadrupole splittings have been obtained by fitting program routines. For the high-temperature cubic phases two crystallographically non-equivalent iron sites have been identified, characteristic of Fe^{2+} in the high-spin state. Abrupt changes of the quadrupole couplings indicated phase transitions; in some cases, the spectra have also revealed several sites for Fe^{2+} in low temperature phases. From the temperature dependences, phase transition temperatures, crystal field splittings and Debye temperatures have been derived.

Key words: ^{57}Fe Mössbauer Spectroscopy; Inorganic Crystals; Structure; Phase Transitions.

1. Introduction

Double sulfates with Langbeinite structure, $A_2B_2(SO_4)_3$ with A = K^+, NH_4^+, Rb^+, Tl^+ and B = Mg^{2+}, Mn^{2+}, Fe^{2+}, Cd^{2+}, have already attracted considerable interest in the past because of their well determined structure with several phase transitions and their remarkable properties. Most compounds of this class undergo structural phase transitions from a paraelectric cubic phase ($P2_13$ symmetric) at room temperature to a ferrelectric orthorhombic phase ($P2_12_12_1$) at low temperatures, sometimes via ferroelectric monoclinic ($P2_1$) and triclinic phases (P1) [1–3]. The phase transitions have been studied using various methods, in particular dielectric [4–10], dilatometric [11], optical [6, 12], Raman [13], heat capacity [14–17], X-ray [7–8, 18], elastic [7, 8, 10] and pyroelectric techniques [9–10].

During the last few years, particular interest has been focused on langbeinites doped with paramagnetic impurity ions such as Cr^{3+}, Mn^{2+} and Fe^{3+} which could be investigated by spectroscopic methods. It was thus possible, especially by electron paramagnetic resonance (EPR), to obtain information on the microstructure in the surroundings of the defect centres and on the phase transitions as well [19–22].

A complementary method, which delivers information on the short range structure of certain probes and which – due to our knowledge – has not yet been applied to Langbeinites so far, is Mössbauer spectroscopy. It is the purpose of the present paper to use ^{57}Fe in iron langbeinites or in other langbeinites doped with Fe^{2+} as a Mössbauer probe to study the incorporation of iron, the environment of iron sites and phase transitions. Information on the spin and oxidation states of iron ions, on structure and phase transitions was obtained, in particular, from isomer shifts and quadrupole couplings.

Reprint requests to Prof. W. Müller-Warmuth, Fax: 02518323441.

2. Experimental

2.1. Sample Preparation

Crystals of double sulfates $A_2B_2(SO_4)_3$ with A = K^+, NH_4^+, Rb^+, Tl^+ and B = Mg^{2+}, Mn^{2+}, Fe^{2+}, Cd^{2+} were prepared from stoichiometric aqueous solutions of the corresponding A_2SO_4 and BSO_4 compounds [1]. Iron langbeinites $A_2Fe_2(SO_4)_3$ contain a sufficient amount of ^{57}Fe in natural abundance. The other materials were doped with Fe^{2+} enriched in ^{57}Fe. We used 93.3% enriched Fe_2O_3 from the Dupont company, dissolved in hot concentrated sulfuric acid. Special attention was paid to reduce Fe^{3+} to Fe^{2+} using Cd metal in contact with platinium producing hydrogen in statu nascendi. A few Mössbauer measurements of Fe^{3+} doped samples were also made.

Manganese and cadmium langbeinites could be obtained as single crystals, magnesium and iron langbei-

0932-0784 / 98 / 0100-0027 $ 06.00 © – Verlag der Zeitschrift für Naturforschung, D-72027 Tübingen

nites as powders. Evaporation at different temperatures under SO_2 atmosphere (to avoid oxidation of Fe^{2+} during the preparation procedure) between 100 °C (Cd-langbeinites), 120 °C (Mg and Mn) and 140 °C (Fe) proved to be most effective. All the samples were annealed for two hours at 200 °C.

Characterization of the samples by X-ray diffraction and comparison with refined structure determinations [2, 23, 24] led to an examination of the quality of the products and to the identification of possible impurities. X-ray powder diagrams revealed from case to case, in agreement with the Mössbauer measurements, small impurities of α-$FeSO_4$ and $FeSO_4 \cdot H_2O$, whose X-ray data are known [25, 26].

The crystalline samples were then ground and poured into the Mössbauer absorber sample holder. In most cases the absorbers contained 0.2–0.4 mg ^{57}Fe cm^{-2} which has proved to be most favourable.

2.2 ^{57}Fe Mössbauer Measurements

The Mössbauer apparatus consisted of a linear arrangement of source, absorber and detector. Commercial ^{57}Co sources of radiation were used, either in a Rh/metal or in a Cr/metal matrix; the shifts relative to α-iron (which served as a reference for the isomer shifts) are +0.11 mm s^{-1} and –0.154 mm s^{-1}, respectively. The velocity scale was calibrated by the Mössbauer spectrum of sodium nitroprusside $Na_2[Fe(CN)_5NO] \cdot 2H_2O$. The absorber temperature was controlled by commercial flow or bath cryostats (Oxford CF500 and MD306); Mössbauer spectra between 4.2 and 300 K were recorded. As γdetector a NaI(Tl) scintillation counter was utilized.

The Mössbauer spectra were evaluated and fitted using home-made program routines on the basis of least squares fits [27, 28]. The errors that will be given further below in the tables are the sum of the random error and a systematic error which was assumed to be ±0.01 mm s^{-1} for the isomer shift δ, the quadrupole splitting ΔE_Q and the linewidth Γ. Phase transitions could be recognized by an abrupt change of the quadrupole splitting parameter and by a variation of the proportions of the Mössbauer spectra.

3. Results

Most spectra contain several quadrupole doublets at room temperatures ("high temperature phase", marked by LH). If no phase transition occurs, the spectra can be continuously pursued to low temperatures with a smooth variation of the Mössbauer parameters. In some diagrams and various tables we present isomer shifts δ and nuclear-quadrupole splittings

$$\Delta E_Q = \frac{1}{2} e^2 qQ \sqrt{1 + \eta^2/3}$$

with eQ and eq being the nuclear quadrupole moment and the maximum component of the electric field gradient (EFG) tensor in its prinicpal axes system, as usual. η is the asymmetry parameter, which cannot be determined separately in this experiment.

In some compounds we observed phase transitions leading to different types of quadrupole doublets at intermediate temperatures (marked by LM) and at low temperatures (marked by LT). Impurity signals (marked by V1 and V2), if present, were identified as already mentioned in Sect. 2.1 and taken into account in the analysis of the spectra.

3.1 Iron Langbeinites

Figure 1 (left and centre) shows the evolution of the Mössbauer spectra upon decreasing temperatures for the potassium compound which is distinguished by several phase transitions. One recognizes two types of doublets at temperatures between 300 and 150 K (LH1 and LH2), and three different types between 145 and 105 K (LM1, LM2, LM3). Below 100 K there are again two doublets (LT1 and LT2) assigned to the low temperature phase being distinguished by large quadrupole splittings. In addition, two types of small impurity components can be seen, identified as $FeSO_4 \cdot H_2O$ (V1) and α-$FeSO_4$ (V2).

No phase transitions were observed for the compounds with A = NH_4, Rb, Tl; the spectra look correspondingly simpler, Fig. 1 shows an example on the right hand side with only one doublet (LH1) at all temperatures. The samples contained the same type of impurities (V1 and V2).

Some data for selected temperatures, as obtained from the fitting procedures, are summarized in Table 1. The isomer shifts turn out to be not much different, whereas the quadrupole splittings change from compound to compound and still more from LH1 to LH2 and upon temperature variation. For $K_2Fe_2(SO_4)_3$, the same type of spectrum can only be observed until about 144 K; corresponding data for the intermediate and low temperature phases are presented in Table 2.

Figures 2 and 3 show for the potassium iron langbeinite the dependence of δ and ΔE_Q on temperature. The behaviour of the isomer shift is very similar for all three

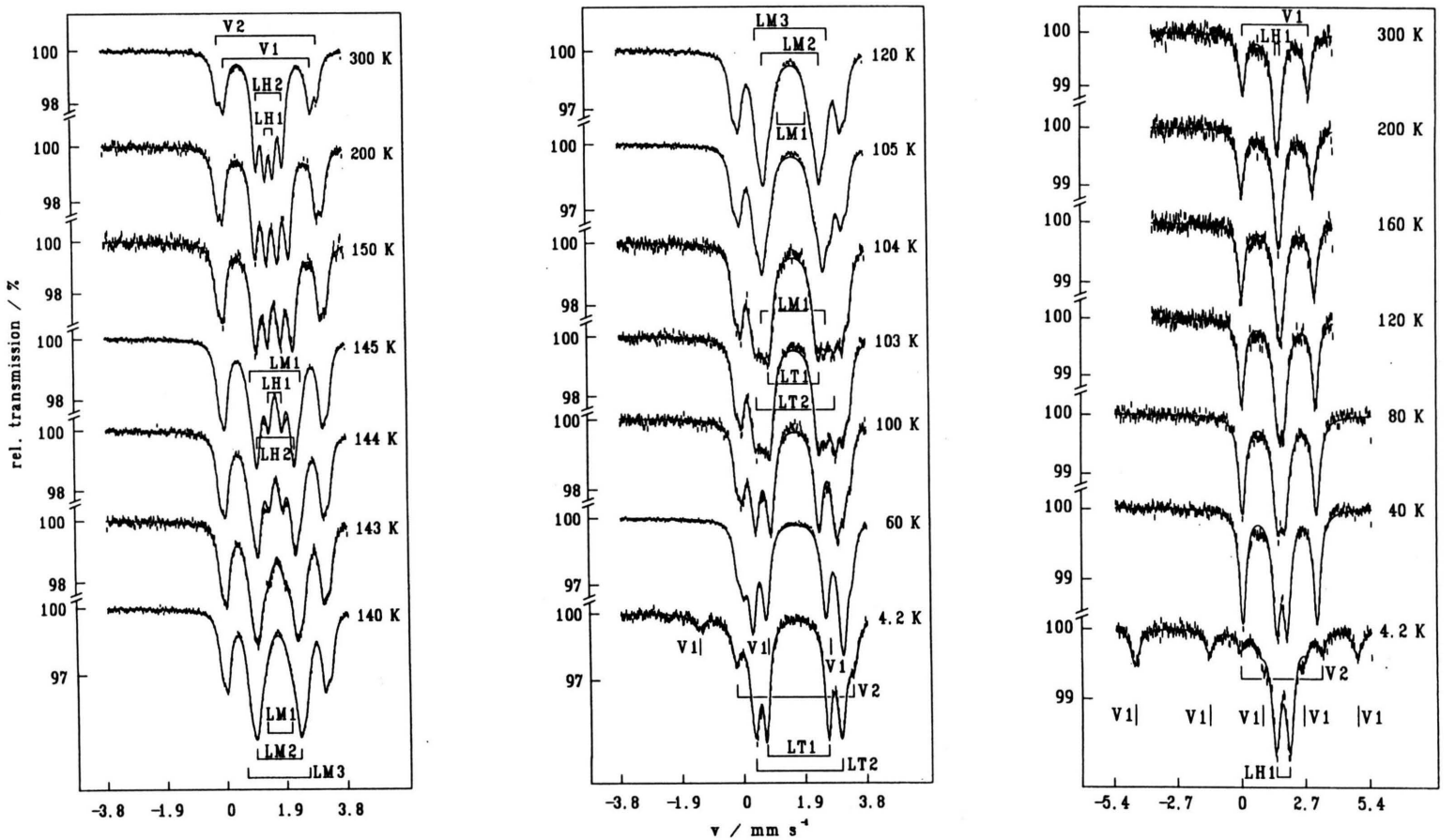

Fig. 1. ^{57}Fe Mössbauer spectra of $K_2Fe_2(SO_4)_3$ (left and centre) and $Tl_2Fe_2(SO_4)_3$ (right), at various temperatures. The abbreviations for the various quadrupole doublets are explained in the text. The solid lines are the result of the fitting procedure.

Table 1. Results obtained from the ^{57}Fe Mössbauer spectra of iron langbeinites $A_2Fe_2(SO_4)_3$ for the cubic phase at various temperatures. LH1 and LH2 correspond to the two separated proportions of the spectra assigned to two non-equivalent sites. Isomer shifts δ and quadrupole splittings ΔE_Q are given in mm/s. Asterisk for A = Rb: the LH2 part could not be identified at 300 K and is given for 200 K.

A	Proportion	300 K		160 K		4.2 K	
		δ	ΔE_Q	δ	ΔE_Q	δ	ΔE_Q
K	LH 1	1.31 (1)	0.25 (2)	1.40 (2)	0.39 (3)	–	–
	LH 2	1.32 (1)	0.84 (2)	1.41 (3)	1.14 (3)	–	–
NH_4	LH 1	1.32 (2)	0.10 (6)	1.38 (2)	0.15 (4)	1.46 (2)	0.26 (2)
	LH 2	1.34 (2)	0.61 (4)	1.43 (2)	1.16 (3)	1.47 (1)	1.95 (2)
Rb	LH 1	1.33 (1)	0.27 (1)	1.42 (1)	0.46 (1)	1.47 (1)	1.03 (2)
	LH 2	1.40 (2)*	0.51 (3)*	1.42 (2)	0.64 (3)	1.47 (2)	1.37 (3)
Tl	LH 1	1.33 (2)	0.1 (1)	1.41 (2)	0.17 (7)	1.46 (2)	0.59 (3)

Table 2. Mössbauer data for the intermediate and low temperature phases of $K_2Fe_2(SO_4)_3$. Arrangement and symbolism as in Table 1.

Proportion	143 K		105 K		100 K		4.2 K	
	δ	ΔE_Q	δ	ΔE_Q	δ	ΔE_Q	δ	ΔE_Q
LM 1	1.40 (4)	0.59 (5)	1.42 (1)	1.37 (3)	–	–	–	–
LM 2	1.41 (2)	1.22 (3)	1.43 (1)	1.84 (2)	–	–	–	–
LM 3	1.42 (2)	1.63 (4)	1.44 (2)	2.30 (3)	–	–	–	–
LT 1	–	–	–	–	1.42 (2)	1.47 (3)	1.45 (2)	1.88 (1)
LT 2	–	–	–	–	1.45 (2)	2.46 (3)	1.48 (2)	2.64 (2)

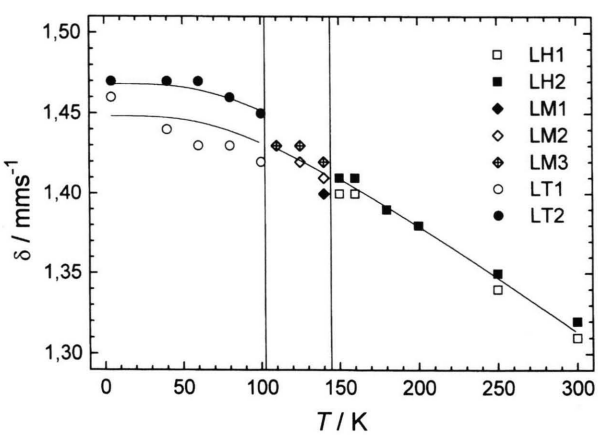

Fig. 2. Temperature dependence of the isomer shifts for $K_2Fe_2(SO_4)_3$. The phase transition temperatures as derived from the Mössbauer spectra are indicated by vertical lines. The connecting lines correspond to a fit by a Debye model with a Debye temperature of 350 K.

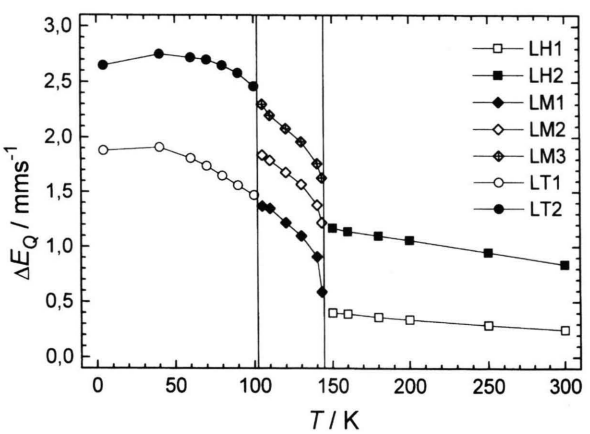

Fig. 3. Temperature dependence of the quadrupole splittings for $K_2Fe_2(SO_4)_3$. The connecting lines are only guides to the eye.

phases, whereas clear abrupt changes can be recognized as far as the quadrupole splitting is concerned. Detailed analysis of the data lead to phase transition temperatures of 145 and 103 K. We discovered one further phase transition at 108.8 K by heat capacity measurements, which, however, did not influence the Mössbauer spectra. The temperature dependences for the other three iron langbeinites are smooth curves over the whole temperature range (not shown) with decreasing values for both δ and ΔE_Q at increasing temperature.

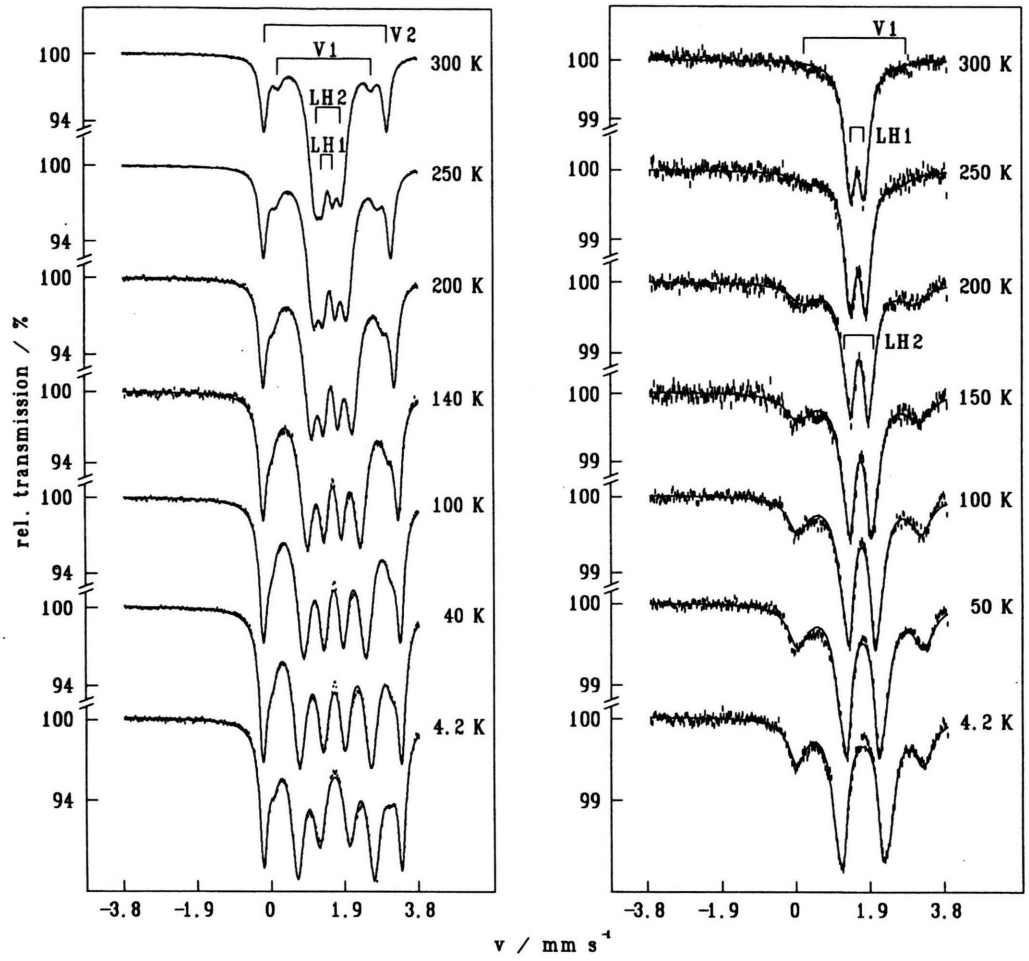

Fig. 4. ^{57}Fe Mössbauer of $(NH_4)_2Mg_2(SO_4)_3$ (left) and $Rb_2Mn_2(SO_4)_3$ at various temperatures.

3.2 Iron Doped Magnesium and Manganese Langbeinites

On the whole, the Mössbauer spectra of the Fe^{2+} doped langbeinites do not look too much different from those of the iron langbeinites. Figure 4 shows two examples. The spectrum of $(NH_4)_2Mg_2(SO_4)_3 : Fe^{2+}$ can well be analyzed in terms of two types of quadrupole doublets LH1 and LH2 and small contributions of impurity spectra V1 and V2. The spectrum of $Rb_2Mn_2(SO_4)_3 : Fe^{2+}$ exemplifies a case where the second contribution LH2 can only be detected at lower temperature. With the exception of both potassium langbeinites, no phase transitions were observed by Mössbauer spectroscopy for the magnesium and manganese langbeinites. For both thallium compounds, only one single contribution LH1 can be seen over the whole temperature range.

We do not present the spectra of $K_2Mg_2(SO_4)_3 : Fe^{2+}$ and $K_2Mn_2(SO_4)_3 : Fe^{2+}$ in detail, since, in principle, they look similar to those of $K_2Fe_2(SO_4)_3$. For B = Mg, a phase transition at 130 K can be identified from the temperature dependence of the Mössbauer spectra, for B = Mn two phase transitions at 188.5 and 180.5 K.

Detailed Mössbauer data are presented in Tables 3 and 4 for the high temperature phase. The low and intermediate temperature phases of both potassium compounds are again distinguished by a smooth transition of the isomer shift and a sudden change in the quadrupole splittings. We do not show a separate table, but a graph of the temperature dependences of ΔE_Q for the various proportions, cf. Figures 5 and 6.

Table 3. Isomer shifts and quadrupole splittings in mms^{-1} as obtained from the Mössbauer spectra of the doped magnesium langbeinites $A_2Mg_2(SO_4)_3 : Fe^{2+}$ with A = K, NH_4, Rb, Tl for the cubic phase at various temperatures.

A	Proportion	300 K		140 K		4.2 K	
		δ	ΔE_Q	δ	ΔE_Q	δ	ΔE_Q
K	LH 1	1.30 (1)	0.36 (2)	1.40 (1)	0.62 (2)	–	–
	LH 2	1.31 (2)	1.14 (3)	1.42 (2)	1.95 (3)	–	–
NH_4	LH 1	1.31 (1)	0.25 (2)	1.41 (1)	0.44 (2)	1.45 (1)	0.77 (1)
	LH 2	1.33 (1)	0.69 (2)	1.43 (1)	1.37 (2)	1.47 (1)	1.96 (1)
Rb	LH 1	1.33 (1)	0.38 (3)	1.42 (2)	0.62 (4)	1.46 (3)	0.93 (5)
	LH 2	1.33 (3)	0.8 (1)	1.43 (3)	1.15 (9)	1.46 (2)	1.51 (5)
Tl	LH 1	1.32 (2)	0.30 (5)	1.40 (4)	0.55 (8)	1.45 (4)	1.01 (6)

Table 4. Isomer shifts and quadrupole splittings in mms^{-1} as obtained from the Mössbauer spectra of the doped manganese langbeinites $A_2Mn_2(SO_4)_3$: Fe^{2+} with A = K, NH_4, Rb, Tl for the cubic phase at various temperatures.

A	Proportion	300 K		200 K		4.2 K	
		δ	ΔE_Q	δ	ΔE_Q	δ	ΔE_Q
K	LH 1	1.31 (2)	0.32 (4)	1.37 (2)	0.59 (5)	–	–
	LH 2	1.33 (2)	0.72 (5)	1.39 (2)	1.00 (5)	–	–
NH_4	LH 1	1.32 (2)	0.15 (5)	1.39 (2)	0.19 (2)	1.45 (2)	0.49 (3)
	LH 2	1.34 (2)	0.52 (7)	1.41 (2)	0.92 (4)	1.46 (2)	1.86 (4)
Rb	LH 1	1.35 (2)	0.35 (2)	1.40 (2)	0.42 (3)	1.47 (2)	0.98 (7)
	LH 2	–	–	1.38 (3)	0.7 (1)	1.48 (2)	1.3 (1)
Tl	LH 1	1.33 (2)	0.34 (3)	1.38 (3)	0.46 (4)	1.45 (5)	1.16 (9)

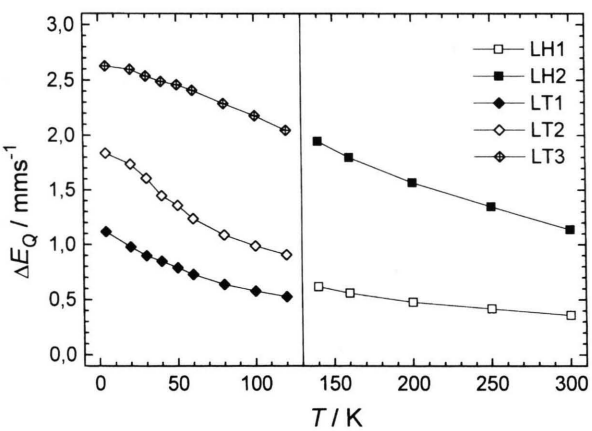

Fig. 5. Temperature dependence of the quadrupole splittings for $K_2Mg_2(SO_4)_3 : Fe^{2+}$. The connecting lines are only guides to the eye.

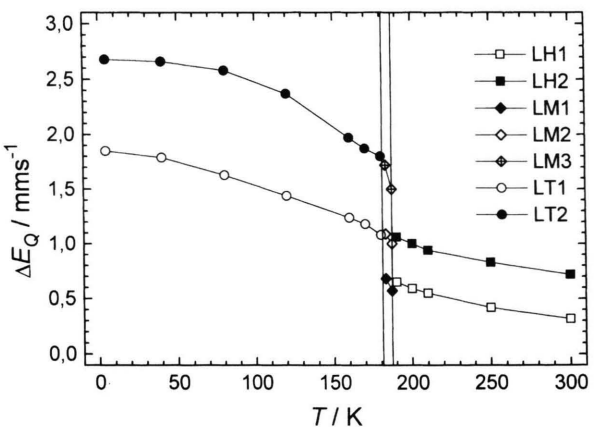

Fig. 6. Same as Fig. 5, but for $K_2Mn_2(SO_4)_3$.

3.3 Iron Doped Cadmium Langbeinites

Mössbauer spectra of $A_2Cd_2(SO_4)_3 : Fe^{2+}$ with A = NH_4, Rb and Tl were studied. Figure 7 shows as an example the spectrum of the ammonium compound where the phase transition at 85 K can well be recognized. We have analyzed the spectra in terms of two quadrupole doublets at high (LH1, LH2) and two doublets at low temperatures (LT1, LT2) and the impurity V1. Figure 8 shows the behaviour of the various quadrupole splittings.

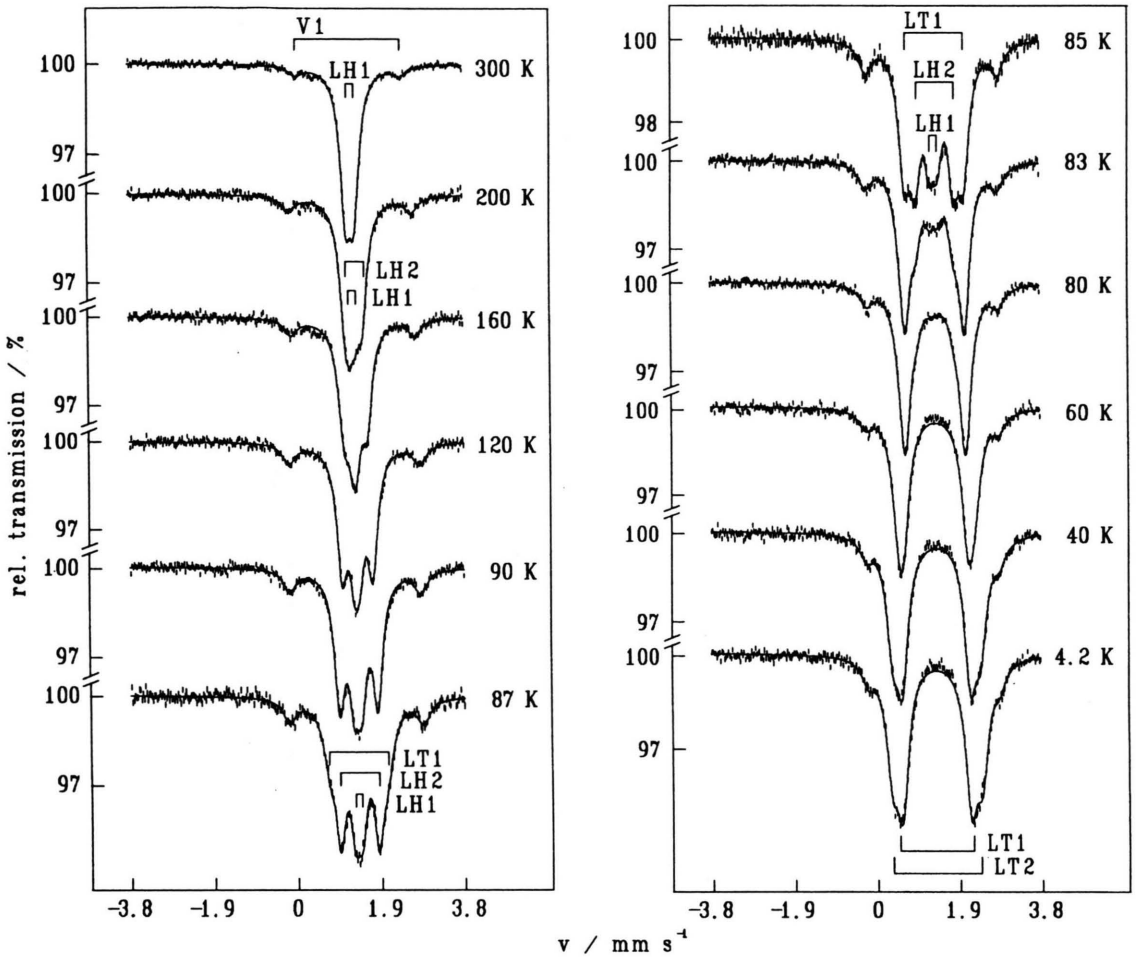

Fig. 7. ^{57}Fe Mössbauer spectra of $(NH_4)_2Cd_2(SO_4)_3 : Fe^{2+}$ at various temperatures. The solid lines are again the result of the fitting procedure.

Table 5. Isomer shifts and quadrupole splittings in mms^{-1} as obtained from the Mössbauer spectra of cadmium langbeinites $A_2Cd_2(SO_4)_3$: Fe^{2+} with A = NH_4, Rb, Tl for the cubic phase at various temperatures.

A	Proportion	300 K		100 K		4.2 K	
		δ	ΔE_Q	δ	ΔE_Q	δ	ΔE_Q
NH_4	LH 1	1.35 (1)	0.19 (2)	1.46 (1)	0.14 (2)	–	–
	LH 2	–	–	1.48 (1)	0.79 (2)	–	–
Rb	LH 1	1.35 (2)	0.20 (5)	1.46 (3)	0.89 (4)	1.47 (2)	1.3 (1)
	LH 2	–	–	–	–	1.50 (5)	2.1 (2)
Tl	LH 1	1.34 (3)	0.20 (7)	1.45 (2)	1.10 (4)	–	–

For the rubidium compound, no phase transition could be observed but the contribution LH2 is only visible at temperatures below 95 K. $Tl_2Cd_2(SO_4)_3 : Fe^{2+}$, finally, reveals a phase transition at 92.5 K; above this point only one proportion LH1 was observed, below the phase transition we found two doublets LT1 and LT2.

Table 5 summarizes some parameters for the high temperature phases. Towards low temperatures, the isomer

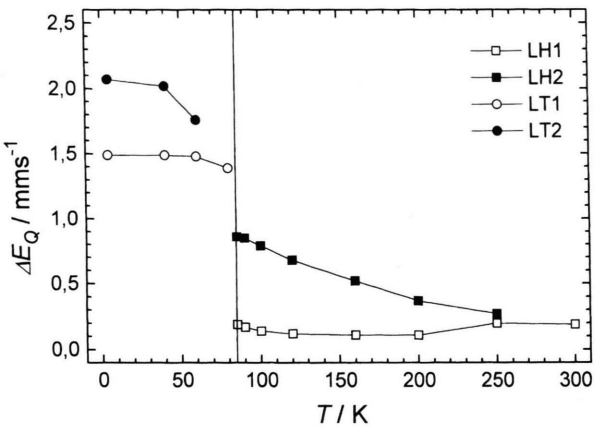

Fig. 8. Temperature dependence of the quadrupole splittings below and above the phase transition temperature of 85 K for $(NH_4)_2Cd_2(SO_4)_3 : Fe^{2+}$. The connecting lines are only guides to the eye.

shifts increase smoothly, even in the presence of phase transitions. The quadrupole splittings, on the other hand, vary abruptly, as shown in Figure 8. For $Tl_2Cd_2(SO_4)_5 : Fe^{2+}$ (not shown), at 4.2 K the splittings amount to 1.51 (6) mm/s (LT1) and 2.05 (8) mm/s (LT2), being clearly larger than those for LH1 (Table 5).

In addition to Fe^{2+} doped samples we carried out some experiments with $(NH_4)_2Cd_2(SO_4)_3 : Fe^{3+}$, especially to compare the results with EPR measurements [20, 22]. The spectra appeared to be less good than those for $(NH_4)_2Cd_2(SO_4)_3 : Fe^{2+}$ because of large linewidths and the unavoidable presence of Fe^{2+}.

4. Discussion

4.1 Isomer Shifts

The observed isomer shifts are all very similar and range from 1.30 to 1.35 mm s^{-1} at room temperature. They are characteristic of Fe^{2+} in the high-spin state. Upon decreasing temperature, there is an increase of δ up to about 1.50 mm s^{-1}, independent of phase transitions which might occur or not. The temperature dependence can be explained in terms of the vibration of the ions on their lattice sites. Figure 2 shows a typical example for this, where the lines correspond to the "second order Doppler shift" with a Debye model for the frequency distribution [29, 30]. More or less the same Debye temperature of 350 K is obtained for all investigated materials, but such a determination of Debye temperatures from Mössbauer isomer shifts is not very accurate, the error being of the order of ±50 K.

The experiments with an Fe^{3+} doped langbeinite (cf. Sect. 3.3) resulted in isomer shifts of 0.48 mm s^{-1}, characteristic of Fe^{3+} in high-spin states. Large linewidths of 0.6 to 1 mm s^{-1} (compared to about 0.3 mm s^{-1}) make the analysis of the spectra more difficult. Distinction of two different sites was not possible.

4.2 Quadrupole Splittings

The observed electric quadrupole interactions at the iron sites are a measure of the asymmetry of the atomic environment; for high-spin Fe^{2+} with its non-spherical orbital electron occupation they are dominated by the valence contribution. This may also be concluded from the experiments with the S-state ion Fe^{3+}, where the valence contribution is formally absent in the high-spin state and where smaller quadrupole splittings were measured indeed.

The temperature dependence of the quadrupole splittings (apart from the phase transitions) can be explained as usual for high-spin Fe^{2+} ions in an octahedral ligand field by a tetrahedral distortion which leads to a partial lifting of the fivefold degeneracy of the t_{2g} orbitals. In case of a compression of the oxygen surroundings along the diagonal axes of the unit cell the energy splitting ε can be described by [31]

$$\Delta E_Q = \Delta E_Q(O) \cdot \frac{1 - \exp(-\varepsilon / kT)}{1 + 2\exp(-\varepsilon / kT)} + \Delta E_Q^{lig}$$

with $\Delta E_Q(O)$ being the valence contribution for $T \to O$ and ΔE_Q^{lig} the (small) contribution from the distorted ligands. For langbeinites in which the temperature dependence of ΔE_Q could be measured between 300 and 4.2 K continuously (not interrupted by phase transitions), the crystal field splitting parameter ε can thus be estimated, cf. Table 6.

Table 6. Crystal field splittings ε/hc in cm^{-1}, estimated from the temperature dependence of the quadrupole splittings for the two non-equivalent sites LH1 and LH2 for the cubic phase of various langbeinites $A_2B_2(SO_4)_3$.

B	A	ε/hc (LH 1)	ε/hc (LH 2)
Fe	NH_4	36 (7)	95 (1)
	Rb	51 (1)	57 (1)
	Tl	31 (4)	
Mg	NH_4	58 (1)	103 (1)
	Rb	89 (5)	130 (10)
	Tl	57 (6)	
Mn	NH_4	43 (4)	92 (2)
	Rb	67 (4)	90 (10)
	Tl	54 (4)	

Inspection of Table 6 shows that ε is greatly determined by the monovalent ions A^+. The distortion of the two iron sites is particularly different and relatively large for small monovalent ions. For larger ions, such as Tl^+, it is difficult or impossible to distinguish between the two sites in the cubic lattice.

4.3 Two Iron Sites in the Cubic Phase

The observed contributions LH1 and LH2 to the Mössbauer spectra of the high temperature phases can immediately be assigned to the two lattice sites of the divalent ions. The crystal structure is well known [1–3]: the langbeinites crystallize in the cubic phase group $P2_13$, and the unit cell contains two non-equivalent sites for the divalent cations along the threefold [111] axes. Both sites are octahedrally surrounded by oxygen atoms from the sulfate, but the first site is large and its surroundings are less distorted.

The ^{57}Fe Mössbauer spectra of the iron langbeinites can be directly related to the two Fe^{2+} sites. The different distortion is described by the small quadrupole splitting of LH1 and the much larger one for LH2 (cf. Table 1). Distinction between the two sites is less clear for compounds with large monovalent cations like Tl^+. The experiments show that the areas of the two proportions of the spectra are equal within the error limits, as to be expected from the structure.

Langbeinites doped with Cr^{3+}, Mn^{2+} and Fe^{3+} were investigated in some detail by EPR [19, 20, 22], and the paramagnetic impurities were found to occupy in all cases divalent lattice sites substitutionally, however with different occupations. It looked probable that Fe^{2+} dopants with an ionic radius similar to that of Mn^{2+} would also occupy divalent sites. Our results on magnesium, manganese and cadmium langbeinites doped with Fe^{2+} confirm this supposition. On the whole, the spectra are similar to those of the iron langbeinites with two proportions of different quadrupole splitting (Tables 3, 4, 5). Exceptions are again the compounds with A = Tl, where no distinction between LH1 and LH2 was possible.

For Mn^{2+} and Fe^{3+} dopants, largely different occupation numbers of the two crystallographically non-equivalent sites were observed by EPR spectroscopy [19, 20, 22]; only for Cr^{3+} the occupation appeared to be more balanced [22]. The present study for Fe^{2+} shows only a slight preference for the larger site. This can be interpreted in terms of the modified relaxation model [19, 22] which considers the combined effects of the relaxation of the surrounding oxygen atoms towards the centre of the dopant defect and the ligand field stabilization. The first effect is favoured for small dopants at larger sites; it explains the preference of the large site for d^5 ions (Mn^{2+}, Fe^{3+}) with their symmetric orbital electron occupation. If there are three d electrons instead of five (Cr^{3+}) or six as for Fe^{2+}, the ligand field stabilization of the unevenly occupied d orbitals has to be considered in addition, and the latter favours the small site.

4.4 Phase Transitions and Low Temperature Phases

Inspection of the Mössbauer spectra and of Tables 1, 3, 4, 5 shows that for iron, magnesium and manganese langbeinites with A = NH_4, Rb, Tl, as well as for the cadmium langbeinite with A = Rb, no phase transitions were observed. The Mössbauer parameters varied smoothly to very low temperatures and were assigned to the cubic phase with space group $P2_13$. This behaviour is in a certain conflict to observations of phase transitions by other techniques for $(NH_4)_2Mn_2(SO_4)_3$ [11, 14, 32] and $Rb_2Cd_2(SO_4)_3$ [8, 10, 11, 18, 22, 33]. But the absence of any abrupt change of Mössbauer parameters means only that the short range environment of the Mössbauer probe Fe^{2+} remains unchanged. Phase transitions which cannot be observed by Mössbauer spectroscopy must be connected with extremely small variations of the coordination spheres of the iron cations.

Table 7. Phase transition temperatures as observed from the temperature dependence of the Mössbauer spectra and their assignment, if possible. Asterisk means: obtained from heat capacity (DSC) rather than Mössbauer measurements.

Compound		Observed Phase Transition Temperatures in K and Assignment				Other Methods (References)
A	B	$P2_13 \rightarrow P2_1$	$P2_1 \rightarrow P_1$	$P1 \rightarrow P2_12_12_1$	?	
K	Fe	144.5	108.8*	103.0		–
K	Mg				130	[34]
K	Mn	188.5		180.5		[11], [13], [35], [36], [37]
NH_4	Cd	85				[11], [13], [14], [22], [38]
Tl	Cd			92.5		[7], [11], [13], [17], [22], [33]

Table 7 summarizes the phase transition temperatures observed within the frame of the present study. The accuracy amounts to about ±2 K; it is composed of the estimated error from the fitting procedure of the spectra and the error of the temperature measurement [±0.5 K]. Most phase transitions occur for the materials with smaller monovalent cations which were also found to be responsibel for large differences in the two non-equivalent lattice sites. The indicated phase transitions for $K_2Fe_2(SO_4)_3$ and $K_2Mg_2(SO_4)_3$ were not yet reported as far as we know, those for the other three compounds were already measured with different techniques.

Following the classification of Hikita et al. [3], we may distinguish between class I, II and III langbeinites. The first class shows all three transitions (cubic → monoclinic → triclinic → orthorhombic), the second class only one transition (cubic → orthorhombic) and the third class none. We assume that the iron, magnesium and manganese langbeinites with A = NH_4, Rb, Tl belong to class III.

$K_2Fe_2(SO_4)_3$, $K_2Mn_2(SO_4)_3$ and (if literature data are considered in addition) all the cadmium langbeinites seem to belong to class I. $K_2Mg_2(SO_4)_3$ cannot yet be classified since the transition at 130 K was detected for the first time and there is disagreement with heat capacity studies [34].

Only two phase transitions were derived from the Mössbauer quadrupole splittings of $K_2Mn_2(SO_4)_3$ and $K_2Fe_2(SO_4)_3$ (cf. Figure 3). For the latter we identified the third transition from monoclinic to triclinic by heat capacity measurements; this phase transition must be connected with minor displacements of atoms in the vicinity of the Mössbauer probes. At intermediate temperatures, four non-equivalent iron sites exist in the monoclinic and eight in the triclinic phases; from the Mössbauer spectra we may distinguish between three lattice sites with occupation 1:2:1, cf. Table 2. In the low temperature orthorhombic phase, again two sites were identified. Immediate assignment to definite lattice sites is not possible because of missing X-ray diffraction data.

For $(NH_4)_2Cd_2(SO_4)_3 : Fe^{2+}$ two iron sites were identified above the phase transition, and also two sites below, (cf. Figs. 6 and 7). The transition temperature of 85 K compares with that of 87 K observed for $(NH_4)_2Cd_2(SO_4)_3 : Fe^{3+}$ by EPR [22]. In ammonium cadmium langbeinite doped with Cr^{3+} this temperature is 90 K [22]; undoped materials studied by various techniques showed a phase transition from $P2_13$ to $P2_1$ between 92 K and 95 K [5, 6, 11, 13, 14, 15, 38]. Expected phase transitions from $P2_1$ to P_1 and from P1 to $P2_12_12_1$ could neither be observed by Mössbauer spectroscopy nor by other methods.

$Tl_2Cd_2(SO_4)_3$ belongs to class I langbeinites as well, all three phase transition temperatures are well known [8–11, 18, 33]. Mössbauer spectra revealed only one of these transitions, namely that at 92 K assigned to $P1 \rightarrow P2_12_12_1$. Only this phase transition is connected with clear changes of the coordination sphere of the divalent cations. Below the transition point, two Fe^{2+} sites can be distinguished, one with a quadrupole splitting larger than that observed above 90 K (cf. Table 5), the other one with a smaller splitting.

Acknowledgement

The authors would like to thank Dr. W. Schnelle, Max-Planck-Institut für Festkörperforschung, Stuttgart, for carrying out and discussing the heat capacity measurements.

[1] G. Gattow and J. Zemann, Z. Anorg. Allg. Chemie 293, 233 (1958).
[2] D. Speer and E. Salje, Phys. Chem. Minerals **13**, 17 (1986) and references therein.
[3] T. Hikita, M. Kitabatake, and T. Ikeda, J. Phys. Soc. Japan **49**, 1421 (1980) and references therein.
[4] F. Jona and R. Pepinsky, Phys. Rev. **103**, 1126 (1956).
[5] H. Ohshima and E. Nakamura, J. Phys. Chem. Solids **27**, 481 (1992).
[6] M. Glogarova and J. Fousek, phys.stat.sol. (a) **15**, 579 (1973).
[7] T. Ikeda and G. Yasuda, Japan. J. Appl. Phys. **14**, 1287 (1975).
[8] T. Hikita, T. Kudo, Y. Chiubachi, and T. Ikeda, J. Phys. Soc. Japan **41**, 349 (1976).
[9] N. Yamada, J. Phys. Soc. Japan **46**, 561 (1979).
[10] M. Maeda, J. Phys. Soc. Japan **49**, 1090 (1980).
[11] M. Kahrizi and M. O. Steinitz, Solid State Commun. **66**, 375 (1988).
[12] B. Brezina and M. Glogarova, phys.stat.sol. (a), **11**, K 39 (1972).
[13] S. Kreske and V. Devarajan, J. Phys. C. **15**, 7333 (1982).
[14] J. I. Arman and J. Boerio-Goates, Ferroelect. **132**, 141 (1992).
[15] V. Franke, M. Glogarova, and E. Hegenbarth, phys.stat.sol (b), **58**, K 69 (1973).
[16] V. Franke, E. Hegenbarth, and B. Brezina, phys.stat.sol (a), **28**, K 77 (1978).
[17] H. Cao, N. K. Dalley, and J. Boerio-Goates, Ferroelect. **146**, 45 (1993).
[18] N. Yamada and S. Kawano, J. Phys. Soc. Japan, **43**, 1016 (1977).
[19] T. Böttjer, G. Lehmann, and M. Stockhausen, Z. Naturforsch. **47a**, 849 (1992).
[20] T. Böttjer and M. Stockhausen, phys. stat. sol (B) **174**, 359 (1992).

[21] T. Böttjer and M. Stockhausen, Z. Naturforsch. **51a**, 1084 (1996)
[22] J. Kastner, B. D. Mosel, and W. Müller-Warmuth, Z. Naturforsch. **51a**, 1123 (1996) and references therein.
[23] H. N. Ng and C. Calvo, Can.J.Chem. **53**, 1449 (1975).
[24] H. Oelkrug, T. Brückel, D. Hohlwein, A. Hoser, and W. Prandl, Phys. Chem. Minerals **16**, 246 (1988).
[25] D. Samaras and J. Coing-Boyat, Bull. Soc. Fr. Mineral Cristallogr. **93**, 190 (1970).
[26] M. Wildner and G. Giester, N. Jb. Minr. Mh. **7**, 296 (1991).
[27] M. Winterer, Thesis, Universität Münster 1989, unpublished.
[28] U. Pegelow, Thesis, Universität Münster 1993, unpublished.
[29] F. Reif, Grundlagen der Physikalischen Statistik und der Physik der Wärme, W. de Gruyter, Berlin 1976.
[30] D. Barb, Grundlagen und Anwendungen der Mössbauerspektroskopie, Akademie-Verlag, Berlin 1980.
[31] T. C. Gibb, Principles of Mössbauer Spectroscopy, Chapman and Hall, London 1976.
[32] T. Hikita, H. Sekiguchi, and T. Ikeda, J. Phys. Soc. Japan **43**, 1327 (1977).
[33] B. Brezina and A. Fouskova, Kristall and Technik **13**, 623 (1978).
[34] J. Boerio-Goates, J. I. Artman, and B. F. Woodfield, Phys. Chem. Minerals **17**, 173 (1990).
[35] N. Yamada, Y. Chubachi, and T. Ikeda, J. Phys. Soc. Japan **45**, 1638 (1978).
[36] J. Boerio-Goates, B. F. Woodfield, and J. I. Artman, Thermochim. Acta **139**, 157 (1989).
[37] T. Ukeda, K. Itoh, and C. Moriyoshi, J. Phys. Soc. Japan **64**, 504 (1995).
[38] S. K. Misra and S. Z. Korczak, J. Phys. C. **19**, 4353 (1986).